NUREG/CR-1540
BNL-NUREG-51231

LUMPED-PARAMETER MODELS FOR TRANSIENT CONDUCTION IN NUCLEAR REACTOR COMPONENTS

WOLFGANG WULFF
Department of Nuclear Energy
Brookhaven National Laboratory
Upton, New York 11973

Manuscript Completed: December 1979
Date Published: June 1980

Prepared for:
OFFICE OF NUCLEAR REGULATORY RESEARCH
U.S. NUCLEAR REGULATORY COMMISSION
WASHINGTON, D.C.
UNDER CONTRACT NO. DE-AC02-76CH00016
FIN A-3014

Available from
GPO Sales Program
Division of Technical Information and Document Control
U.S. Nuclear Regulatory Commission
Washington, D.C. 20555
and
National Technical Information Service
Springfield, Virginia 22161

ABSTRACT

Lumped-parameter models are presented for the prediction of transient conduction in cylinders, plane-parallel slabs, tubes and fuel elements under conditions of small-break loss of coolant accidents and planned transients in nuclear reactor systems. The model accounts for heat generation by fission and decay and by gamma absorption and water reaction.

The models consist of ordinary differential equations, one each for the solid cylinder, the slab and the tube, and two for fuel pellet and clad in the fuel element. The differential equations are derived from the partial differential equation of energy conservation by volume averaging.

The models can be applied to each axial node of a flow passage. The model formulation is particularly suitable for explicit integration over time with high-order integration schemes for ordinary, first-order differential equations.

TABLE OF CONTENTS

LIST OF FIGURES

LIST OF TABLES

NOMENCLATURE

a,b,c	Coefficients of polynomial for temperature profiles in Eqs. (iii), 81 and 82
c	Specific heat in energy balance
D	Common denominator of coefficients for surface temperatures, defined by Eq. 31 for hollow cylinder, Eq. 63 for slab, and Eq. 103 for fuel element
f(r)	Initial temperature distribution
h	Convective heat transfer coefficient
k	Thermal conductivity of solid
m	Profile parameter for heat generation rate, Eq. 114
n	Exponent for heat generation rate, Eq. 114
N_{Bi}	Biot number, hs/k
q'''	Volumetric heat source strength (fission, decay heat, gamma absorption, water reaction, etc.
r	Radial distance
R, R_m	Radius of surface, mean radius of tube
s	Characteristic length, $s = R_2$ for cylinder, $s = R_2-R_1$ for hollow cylinder and slab, $s = R_3-R_2$ for clad
T	Temperature
U_{ij}	Coefficients for initial steady state of fuel element, Table 4
V_i	Coefficients for initial steady state of fuel element, Table 4

Greek Symb 's

α	Thermal diffusivity, $k/(\rho c)$
β_{ij}, β_i	Coefficients for surface temperatures and temperature distributions, defined by Eqs. 19 through 30 for hollow cylinder, Eqs. 38 through 40 for solid cylinder, Eqs. 51 through 62 for slab, Eqs. 105 through 107 for fuel element. See also Tables 1 through 4.
$\gamma_1,\ldots,\gamma_6$	Fixed geometric parameters

δ	Gas gap width, $R_2 - R_1$
λ_i	Ratio of thermal conductivities, $\bar{k}_i/\bar{k}_g$, i = c,f
ξ	Normalized radial coordinate, defined by Eq. 8 for hollow and solid cylinders and slab
τ	Time
$\Omega_1,\ldots,\Omega_5$	Parameters, defined by Eqs. 98 through 102

Subscripts

1,2,3	Surface label
c	Clad
cy	Cylinder
f	Fuel pellet
g	Gas
i	Inside of tube, left side of slab
sl	Slab
o	Fluid, outside of tube and cylinder, right side of slab

$\langle\ \rangle$	Averaging operator, defined by Eq. 5 for tube, cylinder and slab

Superscripted bar implies dependence on averaged temperature only.

1. INTRODUCTION

Transient lateral heat conduction in fuel elements, steam generator tubes, hydraulic duct walls and support structures of simple geometries can frequently be predicted, with computing efficiency and sufficient accuracy, by lumped-parameter conduction models. Lumped-parameter models are developed by the integral method or volume-averaging technique. Their application to diffusion problems has been reviewed by Goodman (1964).

Two distinct lumped-parameter models are required to describe two different phases of transient, one-dimensional conduction. The first phase is the early time span during which a thermal boundary layer advances from the thermally perturbed boundary toward the interior of the solid. This phase ends when the advancing boundary layer meets an unperturbed boundary surface or a second thermal boundary layer. During this phase, the material thickness is greater than the thermal boundary layer thickness; the conducting system is then called thermally thick. The analysis of thermally thick systems is important for fast thermal transients, including periodic heating and cooling processes, whose characteristic time is less than, or of the order of, s^2/α, where s is the characteristic dimension of the system (half-thickness for plane-parallel slab, radius for cylinder and sphere, etc.), and α is its thermal diffusivity*.

This report deals with the second phase of transient conduction, namely, with transients, the characteristic times of which are significantly greater than s^2/α. The analysis presented here is relevant to the investigation of operational transients and of small-break Loss of Coolant Accidents in nuclear

---

* Symbols are defined in the Nomenclature.

reactor systems, that is, to transients which are currently predicted in "non-LOCA" codes such as TWIGL, RAMONA III and IRT.* These transients are characterized by one-dimensional conduction in most solid structures. The one-dimensional temperature profiles have only monotic variations of curvature. An unknown thermal boundary layer thickness does not appear in the analysis. Axial conduction, parallel to the direction of the coolant flow, is not important.

The lumped-parameter models presented here are derived by volume averaging the heat conduction equation. The models satisfy therefore the thermal energy balance on the average over the volume of averaging. Local details of the temperature fields are estimated from postulated temperature profiles which are consistent with the boundary conditions and the mean temperatures as computed from the time-integrals of the averaged conduction equations.

The computing efficiency of the lumped-parameter models stems from the fact that the partial differential equations of lateral heat conduction in r,τ coordinates are replaced by a single ordinary differential equation in τ for every component with significant storage of thermal energy (one for each axial node with coordinate z, if needed). There is one equation for steam generator tubes, pipe walls, support rods, vessel walls, reflectors and shields, and two equations for fuel elements (pellet and clad). Surface temperatures and internal temperatures are computed from explicit algebraic expressions in terms of mean structural and coolant temperatures. Computing speed is achieved by using efficient algorithms for the integration of ordinary differential equations.

---

* The analysis of quenching during reflood, following a large-break LOCA, involves both phases (Ishii 1975, Wulff and Jones 1978).

The computing accuracy of the lumped-parameter models may be estimated to be approximately equal to that achieved by finite difference schemes with three internal nodes for each structural component (at each axial node, if needed). The actual accuracy may be greater, but it should be assessed for each type of transient by comparing selected lumped-parameter results with analytical or accurate finite difference solutions.

The application of lumped-parameter models, as derived by integral methods, is absolutely indispensable in the development of fast-running computer codes.

The lumped-parameter models are developed below in four steps for four different relevant geometries. First is presented the model for the hollow cylinder (tube). The result is first specialized for the solid cylinder (solid rods), and then for the plane-parallel slab (to approximate vessel walls with small curvatures). After that is developed the model for the composite concentric cylinder (fuel element). Finally, the results are summarized for easy reference.

2. MODEL DEVELOPMENTS

2.1 Hollow Cylinder (Tube)

Consider transient one-dimensional heat conduction through a rigid tube, confined between two concentric, right-circular cylinders of radii R_1 and R_2, as shown in Figure 1. The governing equations for heat conduction are the combination of Fourier's law with the energy balance (Eq. 1), the initial condition (Eq. 2), and the boundary conditions (Eqs. 3 and 4) below:

$$\rho c \frac{\partial T}{\partial \tau} = \frac{1}{r} \frac{\partial}{\partial r} \left(rk \frac{\partial T}{\partial r} \right) + q''' \qquad \text{for } R_1 < r < R_2,\ \tau \geq 0 \tag{1}$$

$$T(r,0) = f(r) \qquad \text{for } R_1 \leq r \leq R_2,\ \tau = 0 \tag{2}$$

$$-k \left. \frac{\partial T}{\partial r} \right|_{r=R_1} = h_1 (T_i - T_1) \qquad \text{at } r = R_1,\ \tau \geq 0 \tag{3}$$

$$-k \left. \frac{\partial T}{\partial r} \right|_{r=R_2} = h_2 (T_2 - T_o) \qquad \text{at } r = R_2,\ \tau \geq 0 \tag{4}$$

The symbols, ρ, c, k, h, q''', T, r and τ designate, respectively, density, specific heat and thermal conductivity of the solid tube, convective heat transfer coefficient, volumetric heat generation rate inside the tube wall, temperature, radial distance and time. The subscripts 1 and 2 refer to positions R_1 and R_2. T_i and T_o are the inner and outer coolant temperatures, respectively, which are specified from hydraulics calculations.

Define the averaging operator $\langle\ \rangle$

$$\langle \phi \rangle \triangleq \frac{2}{R_2^2 - R_1^2} \int_{R_1}^{R_2} \phi(r) \cdot r\,dr\ , \tag{5}$$

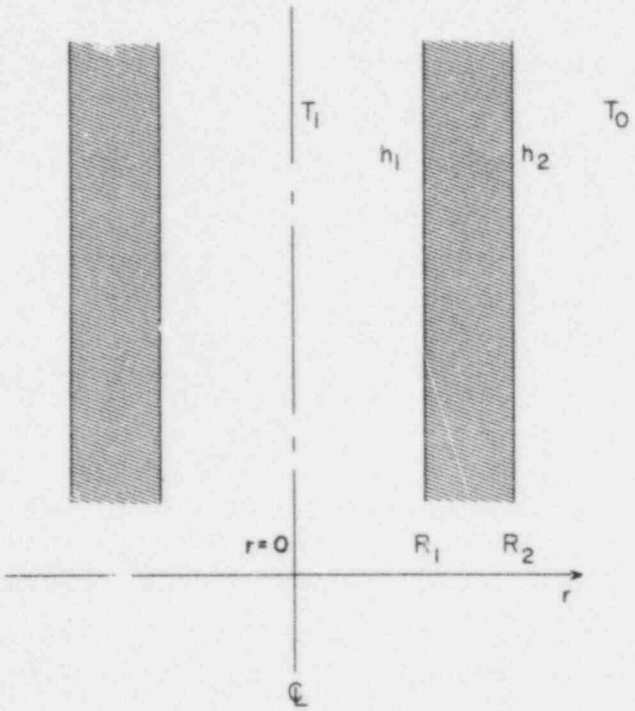

FIGUPE 1. Geometry for Hollow Cylinder

and introduce the simplifications*

$$\text{(i)} \quad \rho(r) \cdot c(r) \equiv \rho c(\langle T \rangle) \quad \underline{\Delta} \; \overline{\rho c}$$

$$\text{(ii)} \quad k(R_1) = k(R_2) = k(\langle T \rangle) \quad \underline{\Delta} \; \bar{k}$$

Apply the operator of Eq. 5 to both sides of Eqs. 1 and 2, use Eqs. 3 and 4 to eliminate the temperature gradients in the averaged conduction equation, and use Assumption (i) to obtain the ordinary differential equation

$$\frac{d\langle T \rangle}{d\tau} = \frac{2\left[R_1 h_1 (T_i - T_1) - R_2 h_2 (T_2 - T_o)\right]}{\overline{\rho c}\,(R_2^2 - R_1^2)} + \frac{\langle q''' \rangle}{\overline{\rho c}} \quad , \tag{6}$$

subject to

$$\langle T \rangle \Big|_{\tau=0} = \langle f(r) \rangle \quad . \tag{7}$$

Equation 6 is exact, except for its limitation by Assumption (i), and can be integrated, subject to Eq. 7, once the surface temperatures T_1 and T_2 are known.

To calculate the surface temperatures T_1 and T_2, we approximate the temperature distribution $T(r)$ in $\left[R_1, R_2\right]$ by a quadratic polynomial which accommodates all available information, as contained in Eqs. 3, 4, and 5:

$$\text{(iii)} \quad T(\xi, \tau) = T_1(\tau) + b(\tau)\xi + c(\tau)\xi^2$$

where

$$\xi \; \underline{\Delta} \; \frac{r - R_1}{R_2 - R_1} = \frac{r - R_1}{s} \quad . \tag{8}$$

The three time-dependent parameters T_1, b and c are determined from three conditions imposed by Eqs. 3, 4 and 5, respectively:

---

* Simplifying assumptions are labelled by Roman numerals; other equations by Arabic numerals.

$$(N_{Bi})_2 T_2 + b + 2c = (N_{Bi})_2 T_o \tag{9}$$

$$(N_{Bi})_1 T_1 - b = (N_{Bi})_1 T_i \tag{10}$$

$$\xi_1 + \gamma_1 b + \gamma_2 c = \langle T \rangle \tag{11}$$

Here, the Biot Numbers $(N_{Bi})_o$ and $(N_{Bi})_i$ are calculated with the aid of Assumption (ii) as $(N_{Bi})_1 \triangleq h_1 s/\bar{k}$ and $(N_{Bi})_2 \triangleq h_2 s/\bar{k}$, where h_1 and h_2 are defined by the instantaneous flow conditions on both sides of the tube wall. The geometric parameters γ_1 and γ_2 are fixed in time and given by

$$\frac{1}{2} \leq \gamma_1 \triangleq \frac{3R_1 + 2s}{3(2R_1 + s)} \leq \frac{2}{3} \quad , \tag{12}$$

$$\frac{1}{3} \leq \gamma_2 \triangleq \frac{4R_1 + 3s}{6(2R_1 + s)} \leq \frac{1}{2} \quad . \tag{13}$$

The lower and upper limits in Eqs. 12 and 13 represent plane-parallel and solid cylindrical geometries, respectively.

The fourth unknown, the outer surface temperature T_2 is obtained from the polynomial (iii) with $\xi = 1$

$$T_1 - T_2 + b + c = 0 \tag{14}$$

Equations 9, 10, 11 and 14 are solved for T_1, T_2 and for a and b. The solution is

$$T_1 = \beta_{11} T_i + \beta_{12} \langle T \rangle + \beta_{13} T_o \quad , \tag{15}$$

$$T_2 = \beta_{21} T_i + \beta_{22} \langle T \rangle + \beta_{23} T_o \quad , \tag{16}$$

$$o = \beta_{31} T_i + \beta_{32} \langle T \rangle + \beta_{33} T_o \quad , \tag{17}$$

$$c = \beta_{41} T_i + \beta_{42} \langle T \rangle + \beta_{43} T_o \quad . \tag{18}$$

The coefficients β_{ij}, i=1,....,4; j=1,....,3, depend on the time-independent geometric parameters γ_1 and γ_2, and on the flow and property-dependent Biot numbers $(N_{Bi})_1$ and $(N_{Bi})_2$:

$$\beta_{11} = (N_{Bi})_1\left[2\gamma_1 - \gamma_2 + (N_{Bi})_2\ (\gamma_1 - \gamma_2)\right]/D \tag{19}$$

$$\beta_{12} = \left[2 + (N_{Bi})_2\right]/D \tag{20}$$

$$\beta_{13} = -\left[\gamma_2 (N_{Bi})_2\right]/D \tag{21}$$

$$\beta_{21} = (N_{Bi})_1\left[2\gamma_1 - \gamma_2 - 1\right]/D \tag{22}$$

$$\beta_{22} = \left[2 + (N_{Bi})_1\right]/D \tag{23}$$

$$\beta_{23} = (N_{Bi})_2\left[1 - \gamma_2 + (N_{Bi})_1\ (\gamma_1 - \gamma_2)\right]/D \tag{24}$$

$$\beta_{31} = -(N_{Bi})_1\left[2 + (N_{Bi})_2\ (1 - \gamma_2)\right]/D \tag{25}$$

$$\beta_{32} = (N_{Bi})_1\left[2 + (N_{Bi})_2\right]/D \tag{26}$$

$$\beta_{33} = -\gamma_2 (N_{Bi})_1\ (N_{Bi})_2/D \tag{27}$$

$$\beta_{41} = (N_{Bi})_1\left[1 + (N_{Bi})_2\ (1 - \gamma_1)\right]/D \tag{28}$$

$$\beta_{42} = -\left[(N_{Bi})_1 + (N_{Bi})_1\ (N_{Ni})_2 + (N_{Bi})_2\right]/D \tag{29}$$

$$\beta_{43} = (N_{Bi})_2\left[1 + \gamma_1\ (N_{Bi})_1\right]/D \tag{30}$$

where

$$D = 2 + (N_{Bi})_2\ (1 - \gamma_2) + (N_{Bi})_1\ (2\gamma_1 - \gamma_2) + (N_{Bi})_1\ (N_{Bi})_2\ (\gamma_1 - \gamma_2)\ . \tag{31}$$

Notice that the evaluation of Eqs. 17, 18 and 25 through 30 is not required for the integration of Eq. 6, but only for the calculation of the temperature profile according to (iii).

Equations 15 through 31 are generally valid for all values of Biot numbers $(N_{Bi})_1$ and $(N_{Bi})_2$. One might expect significant simplifications from specializing Eqs. 19 through 31 for the cases of small Biot numbers.

The Biot numbers $(N_{Bi})_1$ or $(N_{Bi})_2$ are small, respectively, when the thermal resistance to heat transfer in the coolant boundary layer inside or outside the tube overwhelms the thermal resistance in the tube wall. One speaks of Newtonian heating or cooling if both Biot numbers are small compared to unity. Newtonian heating and cooling, $(N_{Bi})_1 << 1$ and $(N_{Bi})_2 << 1$, are characterized by small temperature differences in the solid and large temperature differences in the coolant boundary layers.

After introducing either $(N_{Bi})_1 << 1$, or $(N_{Bi})_2 << 1$, or both of these conditions into Eqs. 19 through 30, one realizes that no significant simplifications are possible in general, because

(a) first-order terms of small Biot numbers must be retained to maintain thermal coupling between fluid(s) and solid and to achieve a steady-state for time-invariant fluid temperatures T_i and T_o and for time-invariant heat generation $\langle q''' \rangle$.

(b) steady-state can be achieved under isothermal conditions, $T_i = \langle T \rangle = T_o$, only if

$$\sum_j \beta_{ij} = \begin{cases} 1 \text{ for } i = 1,2 \\ 0 \text{ for } i = 3,4 \end{cases} .$$

It will be shown in Section 2.2, however, that for the simpler geometry of a solid cylinder, one can achieve simplifications in Eqs. 19 through 30 without violating the constraints (a) and (b) above.

In summary, after evaluating Eqs. 19 through 24 and 31 for the coefficients in Eqs. 15 and 16, one can compute explicitly the surface temperatures T_1 and T_2

as functions only of the mean temperature <T>, the inner coolant temperature T_i, and the outer coolant temperature T_o. With the known surface temperatures T_1 and T_2, one can then integrate Eq. 6 explicitly to obtain future values of the mean temperature <T>. For implicit numerical integration of Eq. 6, the set of Eqs. 15, 16, 19 through 24 and 31, together with the finite-difference form of Eq. 6, become part of the non-linear equation set that describe the channel hydraulics and must be solved iteratively for each time step. In either case, a single ordinary differential equation is integrated to solve the transient conduction problem.

It might be proposed to increase the computing accuracy by extending this method for a model with two or more regions. This is possible in principle; however, each additional region introduces an additional ordinary differential equation for the region mean temperature and three additional unknowns which define the quadratic temperature distribution in the added region. Each one of the three unknowns, in turn, requires three coefficients β_{ij} because the unknowns depend on the three principal temperatures T_i, <T> and T_o. Thus, the number of coefficients rises from six to fifteen and the computing effort more than doubles. As a consequence, the extended model might be a poor contender in the competition with well established collocation methods (Chawla, 1975) which also achieve the increased computing accuracy.

2.2 Solid Cylinder

The results obtained in Section 2.1 for the hollow cylinder can be specialized for the solid cylinder. For this purpose set

$$R_1 = 0 \tag{32}$$

$$s = R_2 \tag{33}$$

$$h_1 = (N_{Bi})_1 = 0 \tag{34}$$

in Eqs. 5, 6, 8, 12, 13, and 19 through 31. Equations 32 and 33 are self-evident, while Eq. 34 implies the appropriate boundary condition $\partial T/\partial r = 0$ at r=0 for a solid cylinder with radial conduction. As expected, Eqs. 32 through 34 yield, after substitution into

$$\left.\begin{aligned} &\text{Eq. 12:} && \gamma_1 = 2/3 \\ &\text{Eq. 13:} && \gamma_2 = 1/2 \end{aligned}\right\} \quad (35)$$

$$\text{Eqs. 19, 22, 25 ÷ 28:} \quad \beta_{11} = \beta_{21} = \beta_{31} = \beta_{32} = \beta_{33} = \beta_{41} = 0 \quad (36)$$

$$\text{Eq. 31:} \quad D = 2 + (N_{Bi})_2/2 \quad (37)$$

$$\left.\begin{aligned} &\text{Eq. 20:} && \beta_{12} = \frac{4 + 2\,(N_{Bi})_2}{4 + (N_{Bi})_2} \\ &\text{Eq. 21:} && \beta_{13} = -\frac{(N_{Bi})_2}{4 + (N_{Bi})_2} \end{aligned}\right\} \quad (38)$$

$$\left.\begin{aligned} &\text{Eq. 23:} && \beta_{22} = \frac{4}{4 + (N_{Bi})_2} \\ &\text{Eq. 24:} && \beta_{23} = -\beta_{13} \end{aligned}\right\} \quad (39)$$

$$\left.\begin{aligned} &\text{Eq. 29:} && \beta_{42} = 2\beta_{13} \\ &\text{Eq. 30:} && \beta_{43} = -\beta_{42} \end{aligned}\right\} \quad (40)$$

With these results, one finds for the centerline temperature

$$T_1 = \frac{\left[4 + 2\,(N_{Bi})_2\right] \langle T \rangle_{cy} - (N_{Bi})_2\, T_o}{4 + (N_{Bi})_2} \quad , \quad (41)$$

for the surface temperature

$$T_2 = \frac{4 \langle T \rangle_{cy} + (N_{Bi})_2\, T_o}{4 + (N_{Bi})_2} \quad , \quad (42)$$

and for the temperature distribution, with $\xi = r/R_2$,

$$T(r,\tau) = \frac{\left[4 + 2(N_{Bi})_2 \ (1 - \xi^2)\right] \langle T\rangle_{cy} - (N_{Bi})_2 \ (1 \quad 2\xi^2) T_o}{4 + (N_{Bi})_2} \ . \tag{43}$$

The time-dependent coolant temperature, T_o, is specified from hydraulics calculations, while the transient mean rod temperature $\langle T\rangle_{cy}$ is defined from Eq. 6 by

$$\frac{d\langle T\rangle_{cy}}{d\tau} = \frac{\langle q''' \rangle_{cy}}{\overline{\rho c}} + \frac{2\overline{k}}{\overline{\rho c}\ R_2^2} \ \frac{4(N_{Bi})_2}{4 + (N_{Bi})_2} \ (T_o - \langle T\rangle_{cy}) \ . \tag{44}$$

and by Eq. 7.

Equations 41 through 44 can be further specified for the cases of Newtonian heating and cooling, which is discussed in Section 2.1. If one ignores second-order terms of $(N_{Bi})_2 << 1$ in Eqs. 41, 42, 43 and 44, then one obtains

$$\left.\begin{aligned}
T_1 &\approx \langle T\rangle_{cy} + (N_{Bi})_2/4\left[\langle T\rangle_{cy} - T_o\right] \\
T_2 &\approx \langle T\rangle_{cy} - (N_{Bi})_2/4\left[\langle T\rangle_{cy} - T_o\right] \\
T(r,\tau) &\approx \langle T\rangle_{cy} + (N_{Bi})_2/4\left[\langle T\rangle_{cy} - T_o\right](1 - 2\xi^2) \\
\frac{d\langle T\rangle}{d\tau} &\approx \frac{\langle q''' \rangle_{cy}}{\overline{\rho c}} - \frac{2\overline{k}}{\overline{\rho c} R_2^2} (N_{Bi})_2 \left[\langle T\rangle_{cy} - T_o\right]
\end{aligned}\right\} \tag{45}$$

In summary, Eqs. 7 and 44 govern the transient mean temperature $\langle T\rangle_{cy}$, Eqs. 41 and 42 define, respectively, the centerline temperature T_1 and the surface temperature T_2, while Eq. 43 defines the internal temperature distribution $T(r,\tau)$ in the solid cylinder with transient radial conduction. The transient conduction problem is solved by integrating a single, ordinary differential equation.

2.3 Plane-Parallel Slab

The results developed in Section 2.1 for a hollow cylinder can also be specialized for a plane-parallel slab, by setting

$$R_1 \to \infty \tag{46}$$

$$R_2 - R_1 = s \tag{47}$$

in Eqs. 5, 6, 8, 12, 13 and 19 through 31. Eq. 5 reduces to

$$\langle \phi \rangle_{sl} = \frac{1}{s} \int_0^s \phi(r) dr \quad . \tag{48}$$

Equation 6 becomes

$$\frac{d\langle T \rangle_{sl}}{d\tau} = \frac{\bar{k}}{s^2 \overline{\rho c}} \left[(N_{Bi})_1 (T_i - T_1) + (N_{Bi})_2 (T_o - T_2) \right] + \frac{\langle q''' \rangle_{sl}}{\overline{\rho c}} \tag{49}$$

Equations 12 and 13 yield, for the slab

$$\gamma_1 = \frac{1}{2} \, , \quad \gamma_2 = \frac{1}{3} \tag{50}$$

Substituting Eq. 50 into Eqs. 19 through 31 gives these results for the coefficients in Eqs. 15 and 16 for T_1 and T_2, respectively:

$$\tilde{\beta}_{11} = (N_{Bi})_1 \left[4 + (N_{Bi})_2 \right] / \tilde{D} \tag{51}$$

$$\tilde{\beta}_{12} = 6 \left[2 + (N_{Bi})_2 \right] / \tilde{D} \tag{52}$$

$$\tilde{\beta}_{13} = -2 (N_{Bi})_2 / \tilde{D} \tag{53}$$

$$\tilde{\beta}_{21} = -2 (N_{Bi})_1 / \tilde{D} \tag{54}$$

$$\tilde{\beta}_{22} = 6 \left[2 + (N_{Bi})_2 \right] / \tilde{D} \tag{55}$$

$$\tilde{\beta}_{23} = (N_{Bi})_2 \left[4 + (N_{Bi})_1 \right] / \tilde{D} \tag{56}$$

and for the coefficients in Eqs. 17 and 18 which define the temperature profile inside the slab:

$$\tilde{\beta}_{31} = -4(N_{Bi})_1 \left[3 + (N_{Bi})_2\right] / \tilde{D} , \tag{57}$$

$$\tilde{\beta}_{32} = 6(N_{Bi})_1 \left[2 + (N_{Bi})_2\right] / \tilde{D} , \tag{58}$$

$$\tilde{\beta}_{33} = -2(N_{Bi})_1 (N_{Bi})_2 / \tilde{D} ; \tag{59}$$

$$\tilde{\beta}_{41} = 3(N_{Bi})_1 \left[2 + (N_{Bi})_2\right] / \tilde{D} , \tag{60}$$

$$\tilde{\beta}_{42} = -6\left[(N_{Bi})_1 + (N_{Bi})_1 (N_{Bi})_2 + (N_{Bi})_2\right] / \tilde{D} , \tag{61}$$

$$\tilde{\beta}_{43} = 3(N_{Bi})_2 \left[2 + (N_{Bi})_1\right] / \tilde{D} ; \tag{62}$$

where

$$\tilde{D} = 12 + 4\left[(N_{Bi})_1 + (N_{Bi})_2\right] + (N_{Bi})_1 (N_{Bi})_2 . \tag{63}$$

With the inner and outer coolant temperatures T_i and T_o computed from the coolant hydraulics, one evaluates first the coefficients β_{ij}, i=1,2, and j=1,2,3, from Eqs. 51 through 56, then the slab surface temperatures T_1 and T_2 from Eqs. 15 and 16, respectively, and from the initial or present mean temperature $\langle T \rangle_{s1}$, either from Eq. 7 or previous integrations, and finally, one integrates Eq. 49 to find future values of the mean temperature $\langle T \rangle_{s1}$. Again, a single ordinary differential equation is integrated to solve the one-dimensional transient conduction problem for the geometry of a plane-parallel slab.

2.4 Fuel Element

Consider transient, axisymmetric radial conduction through the fuel pellet, gas gap and concentric clad as shown in Figure 2. The fuel pellet (subscript f) has the radius R_1, the volumetric heat capacity $(\rho c)_f$, the thermal conductivity k_f, and the volumetric heat generation rate q'''_f (fission or decay heat). The gas

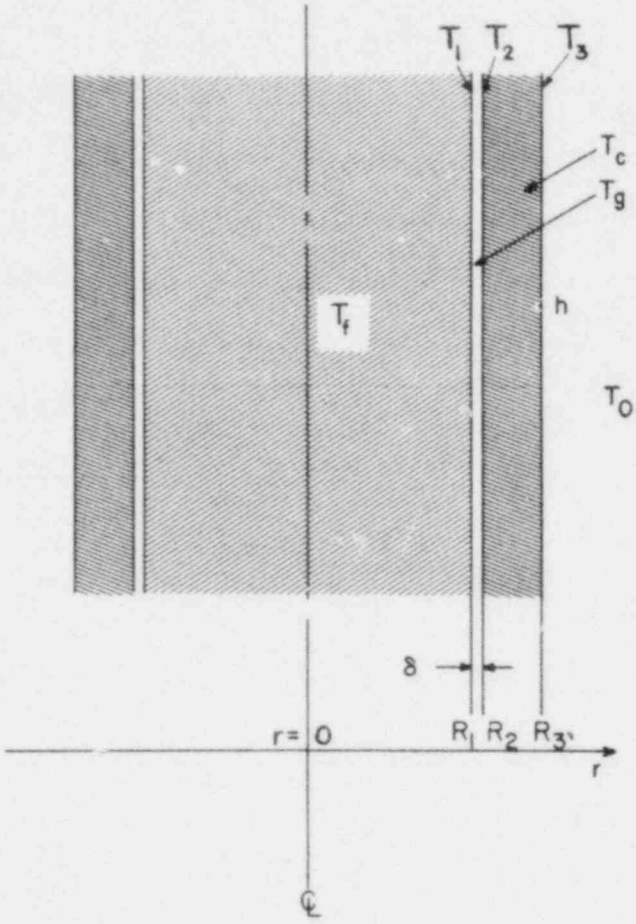

FIGURE 2. Geometry for Fuel Element

in the gas gap (subscript g) between the fuel pellet and the inner clad surface with radius $R_2 = R_1 + \delta$ is taken to have negligible thermal storage capacity and no heat absorption, i.e.,

$$\text{(iv)} \quad (\rho c)_g = 0 \quad ,$$

$$\text{(v)} \quad q'''_g = 0$$

There is no limitation on the relative gap thickness δ/R_1, except that the gas is stagnant and has a thermal conductivity k_g to characterize the heat transfer through the gas. The clad (subscript c) has the inner radius R_2 and the outer radius $R_3 = R_2 + s$, the heat capacity $(\rho c)_c$, the thermal conductivity k_c, and the heat generation rate q'''_c (absorption of gamma radiation and water reaction). The clad is convectively cooled by the fluid with coolant temperature T_o.

The transient radial conduction is governed in the fuel pellet by

$$(\rho c)_f \frac{\partial T_f}{\partial \tau} = \frac{1}{r} \frac{\partial}{\partial r} \left(r k_f \frac{\partial T_f}{\partial r} \right) + q'''_f \quad , \quad 0 \leq r < R_1 \tag{64}$$

$$T_f(r,0) = f_f(r) \quad , \quad 0 \leq r \leq R_1 \tag{65}$$

$$\frac{\partial T_f}{\partial r} = 0 \quad , \quad \text{at } r = 0 \tag{66}$$

$$k_f \frac{\partial T_f}{\partial r} = k_g \frac{\partial T_g}{\partial r} \quad , \quad \text{at } r = R_1 \tag{67}$$

$$T_f(R_1) = T_g(R_1) \triangleq T_1 \quad , \quad \text{at } r = R_1 \tag{68}$$

the gas gap by Eqs. 67 and 68 and by

$$\frac{1}{r} \frac{\partial}{\partial r} \left(r k_g \frac{\partial T_g}{\partial r} \right) = 0 \quad , \quad R_1 < r < R_2 \tag{69}$$

$$k_g \frac{\partial T_g}{\partial r} = k_c \frac{\partial T_c}{\partial r} \quad , \quad \text{at } r = R_2 \tag{70}$$

$$T_g(R_2) = T_c(R_2) \triangleq T_2 \qquad , \text{ at } r = R_2 \tag{71}$$

and in the clad by Eqs. 70 and 71 and by

$$(\rho c)_c \frac{\partial T_c}{\partial \tau} = \frac{1}{r}\frac{\partial}{\partial r}\left(r k_c \frac{\partial T_c}{\partial r}\right) + q'''_c \qquad , R_2 < r < R_3 \tag{72}$$

$$T_c(r,0) = f_c(r) \qquad , R_2 \leq r \leq R_3 \tag{73}$$

$$-k_c \frac{\partial T_c}{\partial r} = h(T_3 - T_o) \qquad , \text{ at } r = R_3 \tag{74}$$

and $$T_3 \triangleq T_c(R_3). \tag{75}$$

The conditions of temperature continuity at the radii $r=R_1$ and R_2, namely, Eqs. 68 and 71, are used here to develop the lumped-parameter conduction model for the fuel element. Alternate conditions can be accommodated with the same method.

Integrating Eq. 69 and using Eqs. 68 and 71 as boundary conditions, one obtains for the gas gap:

$$T_g(r,\tau) = T_1(\tau) - \left[T_1(\tau) - T_2(\tau)\right] \frac{\ln(r/R_1)}{\ln(R_2/R_1)} \tag{76}$$

$$\approx T_1 - (T_1 - T_2)(r-R_1)/\delta \quad \text{for } \delta << R_1$$

and

$$\frac{\partial T_g}{\partial r} = \frac{1}{r}\frac{T_2 - T_1}{\ln(R_2/R_1)} \qquad R_1 \leq r \leq R_2 \ . \tag{77}$$

Combine Assumptions (i) and (ii), namely that the properties $(\rho c)_f = \overline{(\rho c)}_f$ and $k_f \equiv \bar{k}_f$ depend only on the mean temperature $\langle T_f \rangle_f$, with Eq. 64, apply the averaging operator of Eq. 5 with the inner radius equal to zero and the outer radius equal to R_1, use as boundary conditions Eqs. 66 and 67, and evaluate the

latter with the aid of Eq. 77. The result is this ordinary, first-order differential equation for the mean fuel pellet temperature $\langle T_f \rangle_f$:

$$\frac{d\langle T_f \rangle_f}{d\tau} = \frac{2\bar{k}_g}{R_1^2 (\overline{\rho c})_f} \frac{T_1 - T_2}{\ln(R_2/R_1)} + \frac{\langle q''' \rangle_f}{(\overline{\rho c})_f} \quad . \tag{78}$$

Employ Assumptions (i) and (ii) for the clad, i.e., $(\rho c)_c \equiv (\overline{\rho c})_c$ and $k_c \equiv \bar{k}_c$, use the averaging operator of Eq. 5 with the inner radius set equal to R_2 and the outer radius equal to R_3, use the boundary conditions of Eqs. 70 and 74, and evaluate the former with Eq. 77. The result is this ordinary first-order differential equation for the mean clad temperature $\langle T_c \rangle_c$:

$$\frac{d\langle T_c \rangle_c}{d\tau} = - \frac{2R_3 h(T_3 - T_o) + 2\bar{k}_g / \ln(R_2/R_1)(T_2 - T_1)}{(\overline{\rho c})_c s (R_2 + R_3)}$$

$$+ \frac{\langle q''' \rangle_c}{(\overline{\rho c})_c} \tag{79}$$

The two ordinary differential equations, Eqs. 78 and 79, can be integrated, subject to the initial conditions from Eqs. 65 and 73, namely,

$$\langle T_f \rangle_f = \langle f_f \rangle_f \quad \text{and} \quad \langle T_c \rangle_c = \langle f_c \rangle_c \tag{80}$$

as soon as the interfacial temperatures T_1, T_2 and T_3 are known. In order to compute these surface temperatures, we apply Assumption (iii) of Section 2.1 to the fuel and to the clad, and thus find these polynomials for T_f and T_c:

$$T_f(r,\tau) = a_f + b_f(r/R_1) + c_f(r/R_1)^2 \tag{81}$$

$$T_c(r,\tau) = a_c + b_c(r-R_2)/s + c_c\left[(r-R_2)/s\right]^2 \tag{82}$$

where the coefficients a_i, b_i and c_i, $i = f,c$, are functions of time, through their dependence on $\langle T_f \rangle_f$, $\langle T_c \rangle_c$ and T_o.

The three unknown surface temperatures T_1, T_2 and T_3, and the six unknown coefficients a_f, b_f, c_f, a_c, b_c and c_c, are specified by the two conditions that Eqs. 81 and 82 must satisfy the appropriate forms of the averaging operator in Eq. 5 and by the seven boundary conditions as given by Eqs. 66, 67, 68, 70, 71, 74 and 75.

Substituting Eqs. 66, 67 and 68 into Eq. 81 gives

$$b_f = 0 \ , \tag{83}$$

$$T_1 - T_2 + (2\lambda_f \gamma_3) c_f = 0 \ , \tag{84}$$

$$-T_1 + a_f + c_f = 0 \ , \tag{85}$$

where the fixed geometric parameter

$$\gamma_3 \triangleq \ln(R_2/R_1) \approx \delta/R_1 \text{ for } \delta/R_1 << 1 \tag{86}$$

and the property ratio $$\lambda_f \triangleq \overline{k}_f/\overline{k}_s \ . \tag{87}$$

Applying the averaging operator of Eq. 5, with inner radius equal to zero and outer radius equal to R_1, to both sides of Eq. 81 yields

$$2 a_f + c_f = 2\langle T_f \rangle_f \ . \tag{88}$$

Substitute Eq. 70, evaluated with Eq. 77, into Eq. 82. The result is

$$T_1 - T_2 + (\lambda_c \gamma_4) b_c = 0 \ , \tag{89}$$

where the geometric parameter $\gamma_4 \triangleq R_2/s \ \ln(R_2/R_1)$

$$= \gamma_3 R_2/s \tag{90}$$

and the property ratio $$\lambda_c \triangleq \overline{k}_c/\overline{k}_s \ . \tag{91}$$

Substitute Eqs. 71, 74 and 75 into Eq. 82 to obtain

$$T_2 - a_c = 0 \ , \tag{92}$$

$$N_{Bi} T_3 + b_c + 2c_c = N_{Bi} T_o \ , \tag{93}$$

and

$$T_3 - a_c - b_c - c_c = 0 \ . \tag{94}$$

where $N_{Bi} \triangleq hs/\overline{k}_c$ is the Biot number of the clad.

Finally, apply the averaging operator of Eq. 5, with inner radius equal to R_2 and outer radius equal to R_3, to both sides of Eq. 82. The result is analogous to Eq. 11, namely,

$$a_c + \gamma_5 b_c + \gamma_6 c_c = \langle T_c \rangle_c \ , \tag{95}$$

where

$$\gamma_5 \triangleq \frac{3R_2 + 2s}{3(2R_2 + s)} \quad \text{and} \tag{96}$$

$$\gamma_6 \triangleq \frac{4R_2 + 3s}{6(2R_2 + s)} \tag{97}$$

Equations 83 through 85, 88, 89, and 92 through 95 are nine linear equations in the nine unknowns T_1, T_2, T_3, a_f, b_f, c_f, a_c, b_c and c_c. For simplicity, introduce first these six parameters:

$$\Omega_1 \triangleq 4\lambda_f \gamma_3 + 1 \ , \tag{98}$$

$$\Omega_2 \triangleq \gamma_6 - 2\gamma_5 \ , \tag{99}$$

$$\Omega_3 \triangleq 2\lambda_c \gamma_4 \ , \tag{100}$$

$$\Omega_4 \triangleq \Omega_3 (2 + N_{Bi})/2 \ , \tag{101}$$

$$\Omega_5 \triangleq (\Omega_4 - \Omega_3)\gamma_6 \ , \quad \text{and} \tag{102}$$

$$\overline{\overline{D}} \triangleq \Omega_1 \Omega_3 (\Omega_4 - \Omega_5) + (1 - \Omega_1)(\Omega_2 \Omega_4 + \Omega_5) > 0 \ . \tag{103}$$

The fuel pellet surface temperature T_1 is then given by

$$T_1 = \bar{\beta}_1 \langle T_f \rangle_f + \bar{\beta}_2 \langle T_c \rangle_c + \bar{\beta}_3 T_o \ , \tag{104}$$

where

$$\bar{\beta}_1 \triangleq (\Omega_1 - 1)\left[\Omega_4(\Omega_3 - \Omega_2) - \Omega_5(\Omega_3 + 1)\right]/\bar{D} \ , \tag{105}$$

$$\bar{\beta}_2 \triangleq \Omega_5\Omega_4/\bar{D} \ , \text{ and} \tag{106}$$

$$\bar{\beta}_3 \triangleq -\Omega_3\Omega_5/\bar{D} \ . \tag{107}$$

The inner clad surface temperature T_2 is given by

$$T_2 = \langle T_f \rangle_f - \Omega_1\left[\langle T_f \rangle_f - T_1\right] = a_c \ , \tag{108}$$

while the outer clad surface temperature T_3 is computed from

$$T_3 = \left[(\Omega_4 - \Omega_3)T_o - T + (\Omega_3 + 1)T_2\right]/\Omega_4 \tag{109}$$

The temperature profile in the fuel pellet is specified by Eq. 81 with the three coefficients a_f, b_f and c_f given from Eqs. 83, 84 and 85. With the fuel pellet mean and surface temperatures known, one finds for the fuel pellet center line temperature a_f

$$a_f = 2\langle T_f \rangle_f - T_1 \tag{110}$$

and for the remaining two coefficients

$$b_f = 0 \qquad \text{and} \tag{83}$$

$$c_f = -2\left[\langle T_f \rangle_f - T_1\right] \ . \tag{111}$$

The temperature profile in the clad is given by Eq. 82, with a_c defined by Eq. 108, and with

$$b_c = N_{Bi}(T_3 - T_o) - 2(T_2 - T_3) \ , \tag{112}$$

$$c_c = -N_{Bi}(T_3 - T_o) + (T_2 - T_3) \ . \tag{113}$$

The temperature distribution in the gas gap is given by Eq. 76 in terms of the interface temperatures T_1 and T_2 in Eqs. 104 and 108. This completes the description of the transient temperature field in the fuel element.

In summary, two ordinary differential equations, Eqs. 78 and 79, subject to the initial conditions in Eq. 80, must be integrated with respect to time to obtain the two principal variables for the temperature in fuel pellet and clad, namely, the mean temperatures $\langle T_f \rangle_f$ and $\langle T_c \rangle_c$. The third principal variable in the conduction analysis is the coolant temperature T_o and is computed from the coolant hydraulics. The two ordinary differential equations contain the interfacial temperatures T_1, T_2 and T_3, which are explicitly computed from the principal variables $\langle T_f \rangle_f$, $\langle T_c \rangle_c$ and T_o, with the aid of Eqs. 104, 108 and 109 and in terms of six parameters Ω_1, ... , Ω_5 and $\bar{D}$. These parameters depend on geometry, properties and flow conditions, and are defined in Eqs. 98 through 103, and define in turn the coefficients $\bar{\beta}_1$, $\bar{\beta}_2$ and $\bar{\beta}_3$ for the calculation of T_1.

It should be emphasized that Eqs. 81 and 82 are approximations to the exact temperature profiles. However, they encompass all the information contained in the boundary conditions, Eqs. 83 through 85, 89, and 92 through 94, and in the definition of averaging, Eqs. 88 and 95. These conditions apply universally during all transients and during steady state.

The accuracy of the quadratic profile in Eq. 81 can be assessed with the aid of Heisler (Jakob 1958) charts for special transients with sudden change in environmental temperature and without power generation. The Heisler charts apply only to times $\tau > s^2/\alpha$, as does the model presented here. Figure 3 shows a comparison between the exact and the lumped-parameter profiles, both having the same Biot number $hR_1/\bar{k}_f = 20$, the same mean temperature $\langle T_f \rangle_f$, and the same environmental temperature T_2. The curves depict the normalized temperature $(T-T_2)/(\langle T_f \rangle_f - T_2)$ versus the normalized radius (r/R_1). The comparison holds for all

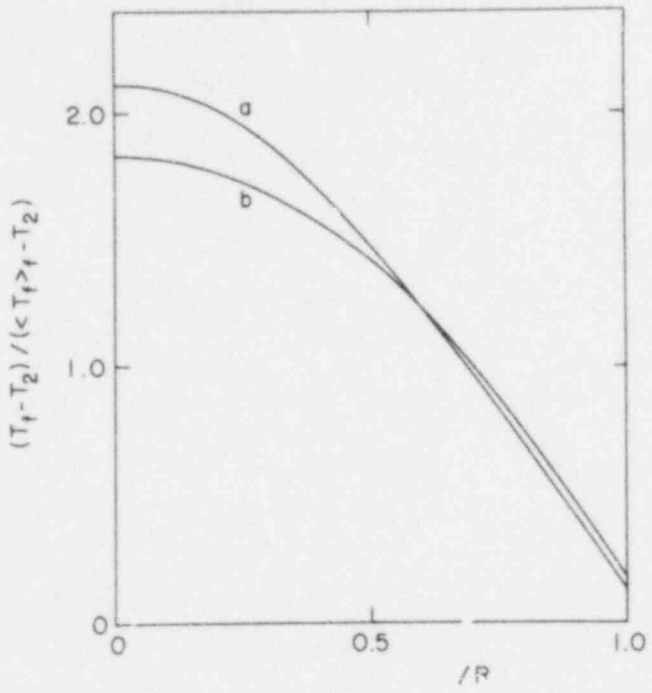

FIGURE 3. Comparison of Temperature Profile from Heisler Charts (Curve a) with Lumped-Parameter Approximation (Curve b)

times $\tau > 2s^2/\alpha$. The selected Biot number is close to the typical Biot number of 24.6 which represents $R_1 = 6.5$ mm, $k = 3\ Wm^{-1}C^{-1}$ (UO_2 at 1000°C), and $h = 11{,}356\ Wm^{-2}C^{-1} \approx 2{,}000$ Btu $hr^{-1}\ ft^{-2}\ F^{-1}$. The agreement deteriorates for higher Biot numbers and improves for lower Biot numbers, but is better than in Figure 3 for typical initial conditions.

The quadratic profile in Eq. 81 is exact for steady state, constant thermal conductivity and uniform power generation. The power generation in fuel pellets is known to be uniform when the fuel is fresh but to concentrate at the pellet periphery after some burnup. In order to account for the non-uniform power distribution, one sets

$$q'''_f(\xi) = \frac{n+2}{n+2(m+1)} \langle q'''_f \rangle_f (1+m\xi^n) \tag{114}$$

with typical values of $m \approx 0.5$, $n = 2$, and extreme limits of $0 \leq m \leq 3$, and $2 \leq n \leq 4$. Fresh fuel is represented by m=0. Figures 4 and 5 show comparisons between exact steady-state profiles and lumped-parameter approximations. The curves are drawn for the same Biot number $N_{Bi} = 24.60$, for the same mean fuel temperature $\langle T_f \rangle_f$, the same mean heat generation rate $\langle q'''_f \rangle_f$, and the same environmental temperature T_2. Figure 4 shows the exact curves for the typical exponent n=2, and the distribution parameter m=0, 0.5, 1, 2 and 3, while Figure 5 shows the same curves for the larger exponent n=4. It is clear that the quadratic profile is sufficiently accurate for typical distribution parameters $0 \leq m \leq 0.5$. It overpredicts the centerline temperature by at most 12%, typically by 4%, and it underpredicts the surface temperature by at most 15%, typically by 2%, all relative to the excess above the environmental temperature T_2.

It may also be interesting to note that the mean temperature does not appear at the midpoint, $\xi = 0.5$, but near $\xi = 1/\sqrt{2} \approx 0.707$. The midpoint assumption is often used in finite differencing schemes with linear radial coordinates. It applies in cylindrical coordinates only to the quadratic coordinate ξ^2.

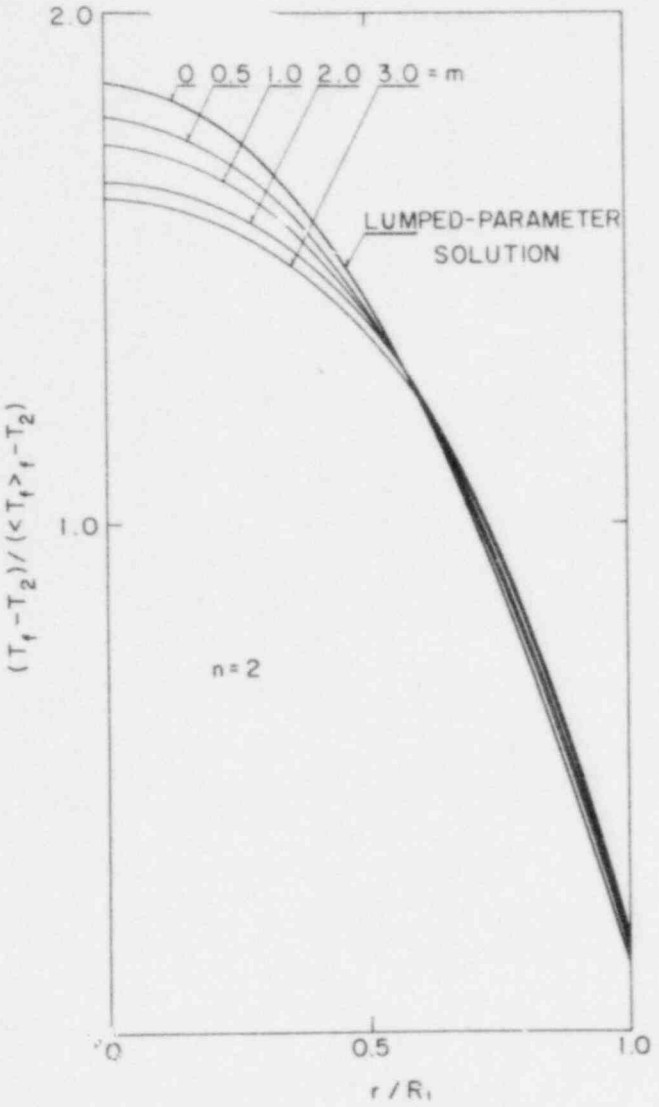

FIGURE 4. Temperature Profiles for Non-uniform Power Generation, Compared with Lumped-Parameter Approximation, n = 2 (See Eq. 114)

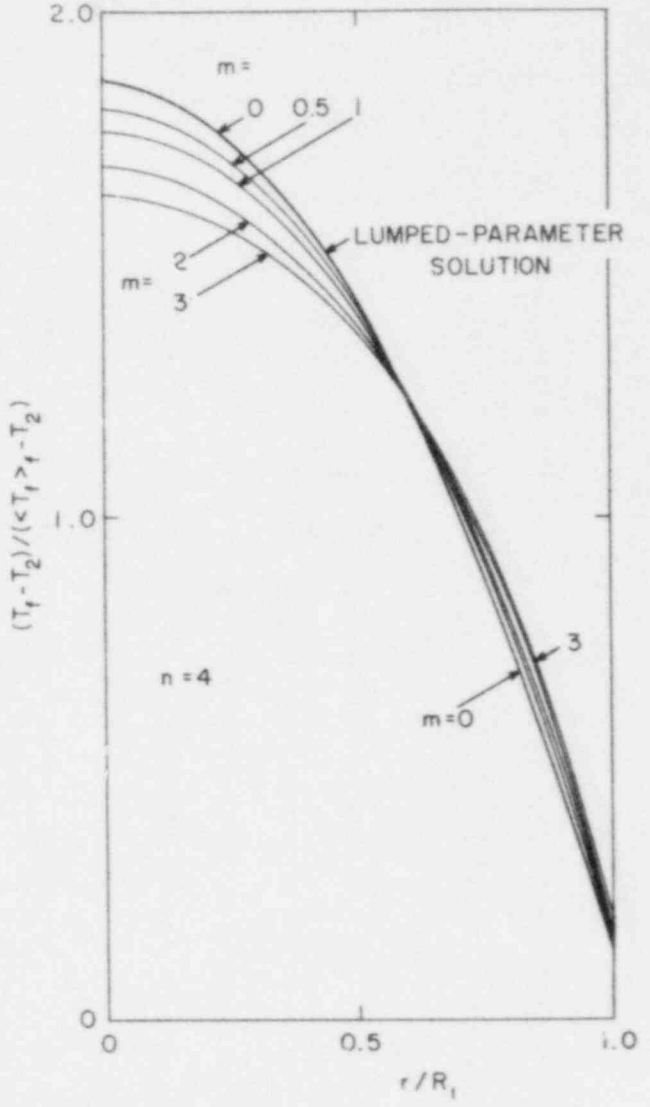

FIGURE 5. Temperature Profiles for Non-uniform Power Generation, Compared with Lumped-Parameter Approximation, n = 4 (See Eq. 114)

3. SUMMARY OF RESULTS

Tables 1 through 4 are a summary of the expressions for computing transient, one-dimensional lateral conduction in sold cylinders, plane-parallel slabs, tubes and nuclear reactor fuel elements consisting of fuel pellet, gas gap and clad.

Included in the tables are also expressions for initial conditions for the special case that the initial state is steady. The initial steady state conditions were derived by setting the time derivatives in the governing equation(s) equal to zero. This method guarantees an initial steady state which is consistent with all the implied hypotheses (i) through (iii). The expressions for the initial values are explicit in the mean temperatures and can be evaluated explicitly from given geometry, thermophysical properties, flow conditions and heating power levels, only if the latter three are temperature independent. In general, the expressions must be evaluated iteratively.

The tables are organized to give first the governing equations, that is, the ordinary differential equations for the principal variables of the temperature fields in the solid. Then follow the appropriate initial steady-state conditions and the important temperatures at the center line (where applicable) and at the surfaces. Next are given the temperature distributions, and finally the definitions for all the coefficients appearing in the preceding expressions. All but the expressions for the initial conditions are explicit in the principal variables (mean temperature in solid and fluid temperatures), geometric parameters and heat generation rate.

TABLE 1. Solid Cylinder

$s = R_2$, $(N_{Bi})_2 = hs/\bar{k}$, $\alpha = \bar{k}/(\overline{\rho c})$, $\xi = r/s$

Governing Differential Equation	$\dfrac{d\langle T\rangle_{cy}}{d\tau} = \dfrac{\bar{\alpha}}{s^2}\dfrac{(N_{Bi})_2(T_o - \langle T\rangle_{cy})}{4 + (N_{Bi})_2} + \dfrac{\langle q''' \rangle_{cy}}{\overline{\rho c}}$
Initial Condition $\tau = 0$ evaluated for steady state	$\langle T\rangle_{cy} = \langle f_{cy}(r)\rangle_{cy} = T_o + \dfrac{\langle q''' (o)\rangle_{cy} s^2}{8\bar{k}}\dfrac{(N_{Bi})_2 + 4}{(N_{Bi})_2}$
Temperature at center line $\xi = 0$	$T_1 = \dfrac{\left[4 + 2(N_{Bi})_2\right]\langle T\rangle_{cy} - (N_{Bi})_2 T_o}{4 + (N_{Bi})_2}$
at surface $\xi = 1$	$T_2 = \dfrac{4\langle T\rangle_{cy} + (N_{Bi})_2 T_o}{4 + (N_{Bi})_2}$
distribution $0 \le \xi \le 1$	$T(r,\tau) = \dfrac{\left[4 + 2(N_{Bi})_2(1-\xi^2)\right]\langle T\rangle_{cy} - (N_{Bi})_2(1-2\xi^2)T_o}{4 + (N_{Bi})_2}$

TABLE 2. Plane-Parallel Slab

$(N_{Bi})_j = h_j s/\bar{k}$, $j = 1,2$; $\alpha = \bar{k}/(\overline{\rho c})$, $\xi = x/s$

Governing Differential Equation	$\dfrac{d\langle T\rangle_{sl}}{d\tau} = \dfrac{\bar{\alpha}}{s^2}\left[(N_{Bi})_1(T_i - T_1) + (N_{Bi})_2(T_o - T_2)\right] + \dfrac{\langle q''' \rangle_{sl}}{(\overline{\rho c})}$
Initial Steady State Condition, at $\tau=0$	$\langle T\rangle_{sl} = \left\{ \dfrac{\langle q'''(o)\rangle_{sl} s^2}{\bar{k}} - T_i\left[(\beta_{11}-1)(N_{Bi})_1 + \beta_{21}(N_{Bi})_2\right] - T_o\left[\beta_{13}(N_{Bi})_1 + (\beta_{23}-1)(N_{Bi})_2\right] \right\} \Big/ \left\{ \beta_{12}(N_{Bi})_1 + \beta_{22}(N_{Bi})_2 \right\}$
Temperature	
at Surface 1 $\xi=0$	$T_1 = \beta_{11} T_i + \beta_{12}\langle T\rangle_{sl} + \beta_{13} T_o$
at Surface 2 $\xi=1$	$T_2 = \beta_{21} T_i + \beta_{22}\langle T\rangle_{sl} + \beta_{23} T_o$
distribution $0 \le \xi \le 1$	$T(x,\tau) = T_1 + b\xi + c\xi^2$

TABLE 2 (Cont'd)

Plane-Parallel Slab

Coefficients

$$\beta_{11} = (N_{Bi})_1\left[4 + (N_{Bi})_2\right]/\tilde{D}$$

$$\beta_{12} = 6\left[2 + (N_{Bi})_2\right]/\tilde{D}$$

$$\beta_{13} = -2(N_{Bi})_2/\tilde{D}$$

$$\beta_{21} = -2(N_{Bi})/\tilde{D}$$

$$\beta_{22} = 6\left[2 + (N_{Bi})_2\right]/\tilde{D}$$

$$\beta_{23} = (N_{Bi})_2\left[4 + (N_{Bi})_1\right]/\tilde{D}$$

$$\tilde{D} = 12 + 4\left[(N_{Bi})_1 + (N_{Bi})_2\right] + (N_{Bi})_1(N_{Bi})_2$$

$$b = \beta_{31}T_i + \beta_{32}\langle T\rangle_{si} + \beta_{33}T_o$$

$$c = \beta_{41}T_i + \beta_{42}\langle T\rangle_{si} + \beta_{43}T_o$$

$$\beta_{31} = -4(N_{Bi})_1\left[3 + (N_{Bi})_2\right]/\tilde{D}$$

$$\beta_{32} = 6(N_{Bi})_1\left[2 + (N_{Bi})_2\right]/\tilde{D}$$

$$\beta_{34} = -2(N_{Bi})_1(N_{Bi})_2/\tilde{D}$$

$$\beta_{41} = 3(N_{Bi})_1\left[2 + (N_{Bi})_2\right]/\tilde{D}$$

$$\beta_{42} = -6\left[(N_{Bi})_1 + (N_{Bi})_1(N_{Bi})_2 + (N_{Bi})_2\right]/\tilde{D}$$

$$\beta_{44} = 3(N_{Bi})_2\left[2 + (N_{Bi})_1\right]/\tilde{D}$$

TABLE 3. Tube

$s = R_2 - R_1$; $(N_{Bi})_j = h_j s/\bar{k}$; $j = 1,2$; $\bar{\alpha} = \bar{k}/(\overline{\rho c})$; $\xi = (r-R_1)/s$;

$\gamma_1 = (3R_1+2s)/\left[3(2R_1+s)\right]$; $\gamma_2 = (4R_1+3s)/\left[6(2R_1+s)\right]$; $R_m = (R_1+R_2)/2$

Governing Differential Equation	$\frac{d\langle T\rangle}{d\tau} = \frac{\bar{\alpha}}{s^2}\left[\frac{R_1}{R_m}(N_{Bi})_1(T_i-T_1) + \frac{R_2}{R_m}(N_{Bi})_2(T_o-T_2)\right] + \frac{\langle q'''\rangle}{(\overline{\rho c})}$
Initial Steady-State Condition, at $\tau=0$	$\langle T\rangle = \left\{\frac{\langle q'''(o)\rangle s^2}{\bar{k}} - \frac{R_1}{R_m}(N_{Bi})_1\left[(\beta_{11}-1)T_i+\beta_{13}T_o\right] - \frac{R_2}{R_m}(N_{Bi})_2\left[\beta_{21}T_i+(\beta_{23}-1)T_o\right]\right\} \Big/ \left\{\frac{R_1}{R_m}(N_{Bi})_1\beta_{12} + \frac{R_2}{R_m}(N_{Bi})_2\beta_{22}\right\}$
Temperature	
at inner surface $r=R_1$, $\xi=0$	$T_1 = \beta_{11}T_i + \beta_{12}\langle T\rangle + \beta_{13}T_o$
at outer surface $r=R_2$, $\xi=1$	$T_2 = \beta_{21}T_i + \beta_{22}\langle T\rangle + \beta_{23}T_o$
distribution $0 \le \xi \le 1$	$T(\xi,\tau) = T_1 + b\xi + c\xi^2$

TABLE 3 (Cont'd)

Tube

Coefficients

$\beta_{11} = (N_{Bi})_1\left[2\gamma_1 - \gamma_1\gamma_2(N_{Bi})_2\right]/D$	$\beta_{21} = (N_{Bi})_1\left[2\gamma_1 - \gamma_2 - 1\right]/D$
$\beta_{12} = \left[2 + (N_{Bi})_2\right]/D$	$\beta_{22} = \left[2 + (N_{Bi})_1\right]/D$
$\beta_{13} = -\gamma_2(N_{Bi})_2/D$	$\beta_{23} = (N_{Bi})_2\left[1-\gamma_2+(\gamma_1-\gamma_2)(N_{Bi})_1\right]/D$

$$D = 2 + (1-\gamma_2)(N_{Bi})_2 + (2\gamma_1-\gamma_2)(N_{Bi})_1 + (\gamma_1-\gamma_2)(N_{Bi})_1\,(N_{Bi})_2$$

$$b = \beta_{31}T_i + \beta_{32}\langle T\rangle + \beta_{33}T_o$$

$$c = \beta_{41}T_i + \beta_{42}\langle T\rangle + \beta_{43}T_o$$

$\beta_{31} = -(N_{Bi})_1\left[2+(1-\gamma_2)(N_{Bi})_2\right]/D$	$\beta_{41} = (N_{Bi})_1\left[1+(1-\gamma_1)(N_{Bi})_2\right]/D$
$\beta_{32} = (N_{Bi})_1\left[2+(N_{Bi})_2\right]/D$	$\beta_{42} = -\left[(N_{Bi})_1+(N_{Bi})_1(N_{Bi})_2+(N_{Bi})_2\right]/D$
$\beta_{33} = -\gamma_2(B_{Bi})_1(N_{Bi})_2/D$	$\beta_{43} = (N_{Bi})_2\left[1+\gamma_1(N_{Bi})_1\right]/D$

TABLE 4. Fuel Element

Fuel pellet (f): R_1; Gas Gap (g): $\delta = R_2 - R_1$; Clad (c): $s = R_3 - R_2$; $R_m = (R_2 + R_3)/2$; $N_{Bi} = \frac{hs}{\bar{k}_c}$

Governing Differential Equations	$$\frac{d\langle T_f\rangle_f}{d\tau} = \frac{\langle q'''_f\rangle_f}{(\overline{\rho c})_f} - \frac{2\bar{k}_g}{R_1^2(\overline{\rho c})_f}\,\frac{T_1 - T_2}{\ln(R_2/R_1)}$$ $$\frac{d\langle T_c\rangle_c}{d\tau} = \frac{\langle q'''_c\rangle_c}{(\overline{\rho c})_c} + \frac{\bar{k}_g}{R_m s(\overline{\rho c})_c}\,\frac{T_1 - T_2}{\ln(R_2/R_1)} + \frac{R_3}{R_m}\,\frac{\bar{\alpha}_c}{s^2}\,N_{Bi}(T_o - T_3)$$
Initial Steady-State Conditions ($\tau = 0$)	$$\langle T_f\rangle_f = (V_1U_{22} - V_2U_{12})/(U_{11}U_{22} - U_{12}U_{21})$$ $$\langle T_c\rangle_c = (V_2U_{11} - V_1U_{21})/(U_{11}U_{22} - U_{12}U_{21})$$ $$U_{11} = \left\{(1+\Omega_3)\left[1+\Omega_1(\bar{\beta}_1 - 1)\right] - \bar{\beta}_1\right\}/\Omega_4 \qquad U_{12} = \left[(1+\Omega_3)\Omega_1 - 1\right]\bar{\beta}_2/\Omega_4$$ $$U_{21} = (1-\Omega_1)(\bar{\beta}_1 - 1) \qquad U_{22} = (1-\Omega_1)\bar{\beta}_2$$ $$V_1 = \frac{s/R_m}{N_{Bi}}\left[\frac{R_1^2\langle q'''_f(o)\rangle_f}{2\bar{k}_c} + \frac{R_m s\langle q'''_c(o)\rangle_c}{\bar{k}_c}\right] + \frac{\Omega_3 - \bar{\beta}_3\left[(1+\Omega_3)\Omega_1 - 1\right]}{\Omega_4}\,T_o$$ $$V_2 = \frac{R_1^2\langle q'''_f(o)\rangle_f}{2\bar{k}_g}\,\ln\frac{R_2}{R_1} - \bar{\beta}_3(1-\Omega_1)T_o$$

TABLE 4 (Cont'd)

Fuel Element

Temperature at pellet surface $r = R_1$	$T_1 = \overline{\beta}_1 \langle T_f \rangle_f + \overline{\beta}_2 \langle T_c \rangle_c + \overline{\beta}_3 T_o$
at pellet center $r = 0$	$a_f = 2\langle T_f \rangle_f - T_1$
at inner clad surface $r = R$	$T_2 = \langle T_f \rangle_f - \Omega_1 \left[\langle T_f \rangle_f - T_1 \right]$
at outer clad surface	$T_3 = \left[(\Omega_4 - \Omega_3) T_o - T_1 + (\Omega_3 + 1) T_2 \right] / \Omega_4$
Temperature Distribution in fuel pellet $0 \leq r \leq R_1$	$T_f = a_f + c_f (r/R_1)^2$
in clad $R_2 \leq r \leq R_3$	$T_c = T_2 + b_c (r-R_2)/s + c_c \left[(r-R_2)/s \right]^2$
in gas gap $R_1 \leq r \leq R_2$	$T_g = T_1 - (T_1 - T_2) \ln(r/R_1) / \ln(R_2/R_1)$

TABLE 4 (Cont'd)

Fuel Element

Coefficients $\lambda_f = \overline{k}_f/\overline{k}_g$; $\lambda_c = \overline{k}_c/\overline{k}_g$; $\gamma_3 = \ln \frac{R_2}{R_2}$; $\gamma_4 = \gamma_3 R_2/s$

$\gamma_5 = (3R_2+2s)/\left[3(2R_2+s)\right]$; $\gamma_6 = (4R_2+3s)/\left[6(2R_2+s)\right]$

$\Omega_1 = 4\lambda_f\gamma_3 + 1$

$\Omega_2 = \gamma_6 - 2\gamma_5$

$\Omega_3 = 2\lambda_c\gamma_4$

$\Omega_4 = \Omega_3(2 + N_{Bi})/2$

$\Omega_5 = (\Omega_4 - \Omega_3)\gamma_6$

$\overline{D} = \Omega_1\Omega_3(\Omega_4 - \Omega_5) + (1 - \Omega_1)(\Omega_2\Omega_4 + \Omega_5)$

$\overline{\beta}_1 = (\Omega_1 - 1)\left[\Omega_4(\Omega_3 - \Omega_2) - \Omega_5(\Omega_3 + 1)\right]/\overline{D}$

$\overline{\beta}_2 = \Omega_3\Omega_4/\overline{D}$

$\overline{\beta}_3 = -\Omega_3\Omega_5/\overline{D}$

REFERENCES

Chawla, T. C. et al. (1975), "The Application of the Collocation Method Using Hermite Cubic Splines to Nonlinear Transient One-Dimensional Heat Conduction Problems," ASME Trans. J. of Heat Transfer, 97, Ser. C, No. 4, 562-569.

Goodman, T. R. (1964), "Integral Methods for Nonlinear Heat Transfer," in Advances in Heat Transfer, T. F. Irvine, Jr. and J. P. Hartnett, eds., Vol. 1, 51-122, Academic Press.

Ishii, M. (1975), "Study on Emergency Core Cooling," J. Br. Nucl. Energy Soc., 14, July, No. 3, 237-242.

Jakob, M. (1958), Heat Transfer, Vol. 1, pg. 289, John Wiley & Sons, Inc., London.

Wulff, W. and Jones, O. C., Jr. (1978), "THOR-1 (PWR): A Computer Code for Predicting the Thermal Hydraulic Behavior of Nuclear Reactor Systems," Informal Report, Brookhaven National Laboratory, Upton, N. Y., BNL-NUREG-24760, Vol. 2, p. 2.7.1.